Rea, D.K., Basov, I.A., Scholl, D.W., and Allan, J.F. (Eds.), 1995
Proceedings of the Ocean Drilling Program, Scientific Results, Vol. 145

22. GEOCHEMISTRY AND $^{40}Ar/^{39}Ar$ GEOCHRONOLOGY OF BASALTS FROM ODP LEG 145 (NORTH PACIFIC TRANSECT)[1]

Randall A. Keller,[2] Robert A. Duncan,[2] and Martin R. Fisk[2]

ABSTRACT

Leg 145 of the Ocean Drilling Program recovered basalts at three locations in the North Pacific. Drilling at Sites 883 and 884 on Detroit Seamount, near the northern end of the Emperor seamount chain, penetrated altered pillow basalts that may be of transitional composition (Site 883) and thick flows of tholeiitic composition (Site 884). The Site 883 basalts did not yield a reliable crystallization age, but a basalt from Site 884 yielded an age of 81 Ma. This is the first reliable radiometric age determination for the northern end of the Emperor Seamounts, and lengthens the period of known activity of the Hawaiian-Emperor seamount chain by approximately 15 million years. Published Pacific-plate-motion models predict an age for Detroit Seamount of approximately 65 to 75 Ma. Either the 81 Ma tholeiite is from very early in the history of an unusually long-lived volcano, or the velocity of the Pacific plate relative to the Hawaiian hotspot increased some time between 81 and 65 Ma.

Drilling at Site 885 was expected to reach Lower? Cretaceous oceanic crust near the Chinook Trough in the central North Pacific. Basalt was contacted beneath less than one-half of the expected thickness of sediments. The basalt is altered, but appears to have a mid-ocean ridge tholeiite composition. It yielded a concordant $^{40}Ar/^{39}Ar$ plateau age of only 80 Ma, suggesting that volcanism associated with the Late Cretaceous plate reorganization and formation of the Chinook Trough affected a wider area than previously thought.

Drilling at Site 887 on the Patton-Murray seamount platform in the Gulf of Alaska recovered transitional basalts overlain by two chemically distinct types of alkalic basalts. The Site 887 basalts are chemically similar to samples dredged from other seamounts in the northeast Pacific. $^{40}Ar/^{39}Ar$ dating of an alkalic basalt midway in the section yielded an age of 27 Ma. The uppermost basalt recovered is a sediment-bounded sill that yielded an $^{40}Ar/^{39}Ar$ age of 17 Ma. Thus, volcanic activity at this seamount platform spanned at least 10 million years.

INTRODUCTION

Leg 145 of the Ocean Drilling Program (ODP) sampled basalts at the old ends of two seamount chains in the North Pacific. Sites 883 and 884 penetrated basalt at two locations on Detroit Seamount, at the northern end of the Hawaiian-Emperor Seamounts (Fig. 1). Before this expedition, no samples suitable for radiometric dating existed from the Emperor Seamounts north of Suiko Seamount (750 km south of Detroit Seamount). Basalts recovered from Meiji Seamount (which is the only Emperor seamount older than Detroit Seamount and lies 240 km to the northwest) during Leg 19 of the Deep Sea Drilling Project (DSDP) did not yield a reliable $^{40}Ar/^{39}Ar$ age (Dalrymple et al., 1980). The best age constraint for Meiji was a minimum age of 70 Ma, based on biostratigraphic data from the overlying sediments (Worsley, 1973). Leg 145 also recovered basalts at Site 887 on the Patton-Murray seamount platform, the northern end of a prominent linear seamount chain in the Gulf of Alaska (Fig. 1). Patton-Murray seamount platform had previously been dredged and radiometrically dated (Dalrymple et al., 1987).

Leg 145 also drilled to basalt in the north-central Pacific near the Chinook Trough (Fig. 1). The Chinook Trough is thought to be a spreading center that was last active during a plate reorganization at approximately 82 Ma (Rea and Dixon, 1983). Based upon site survey geophysical data, drilling was expected to penetrate approximately 150 m of Tertiary and Cretaceous sediments and bottom in Lower? Cretaceous oceanic crust.

SAMPLE DESCRIPTIONS

Site 883

Drilling at the two basement holes at Site 883 penetrated 24 m and 38 m of basalt at locations approximately 20 m apart, and recovered a series of fractured and altered basalt pillows and flows (Rea, Basov, Janecek, Palmer-Julson, et al., 1993). Numerous lithologic units were identified aboard ship, but this was based almost entirely upon the presence of glassy margins rather than observable lithologic differences. The majority of the samples contain 10%–15% plagioclase microphenocrysts, with minor amounts of altered olivine microphenocrysts. Seven samples were selected for X-ray fluorescence (XRF) analyses from a range of depths below seafloor in the two holes. Two of these seven samples were selected for $^{40}Ar/^{39}Ar$ dating. There were no significant macroscopic differences among the samples.

Site 884

Drilling at Hole 884E penetrated 87 m into basement and recovered basaltic pillows and massive flows (Rea, Basov, Janecek, Palmer-Julson, et al., 1993). Aboard the *JOIDES Resolution* these were divided into 13 lithologic units, based upon the presence of chilled margins or changes in crystallinity. These units fall into three general lithologic groups: (1) aphyric, massive (up to 30 m thick) basalt flows (Units 1, 6, and 7); (2) moderately to highly plagioclase-phyric to megaphyric, massive (up to 6.5 m thick) basalt flows (Units 2–5 and 8–10); and (3) highly plagioclase- to plagioclase-olivine-phyric pillow basalts (Units 11–13). Two representative samples from each of these three groups were chosen for XRF analyses, and one sample each from two of the groups was used in $^{40}Ar/^{39}Ar$ incremental heating experiments.

[1] Rea, D.K., Basov, I.A., Scholl, D.W., and Allan, J.F. (Eds.), 1995. *Proc. ODP, Sci. Results,* 145: College Station, TX (Ocean Drilling Program).

[2] College of Oceanic and Atmospheric Sciences, Oregon State University, Oceanography Admin. Bldg. 104, Corvallis, OR 97331–5503, U.S.A.

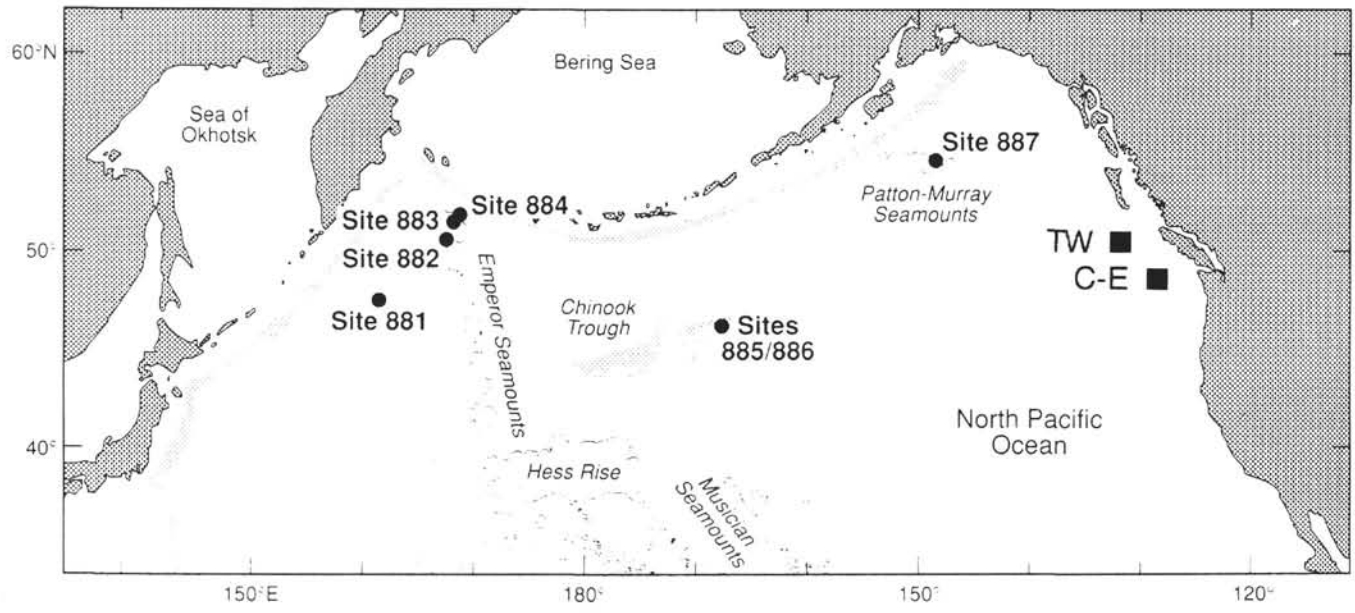

Figure 1. Map of the North Pacific Ocean showing the locations of Leg 145 drill sites (modified from Rea, Basov, Janecek, Palmer-Julson, et al., 1993). Locations for Tuzo Wilson Seamounts (TW) and Cobb-Eickelberg Seamounts (C-E) are shown for comparison to Site 887 (see text).

Site 885

Drilling at Sites 885 and 886 encountered basalt after coring less than one-half of the anticipated 150 m of sediment (Rea, Basov, Janecek, Palmer-Julson, et al., 1993). Approximately 60 cm of angular cobbles of altered, aphyric basalt were recovered at each site. The Site 885 basalt was in slightly larger fragments and appeared less altered, so it was chosen for shore-based XRF and $^{40}Ar/^{39}Ar$ analyses.

Site 887

Drilling at Site 887 penetrated 87 m beneath the first basalt, and recovered 16 m of highly clinopyroxene-plagioclase-phyric to sparsely plagioclase-phyric basalts ranging from massive flows to cobbles that may be pillow fragments (Rea, Basov, Janecek, Palmer-Julson, et al., 1993). Aboard the *JOIDES Resolution,* the basalts were divided into five lithologic units, and six representative samples from four of these units were selected for shore-based XRF analyses; two of these were selected for $^{40}Ar/^{39}Ar$ analyses.

METHODS

Normally, basalt samples are analyzed in the X-ray fluorescence laboratory aboard the *JOIDES Resolution* for major and trace element concentrations, but technical problems and rough seas limited the shipboard analyses to trace elements in samples from Sites 883 and 884 only (Rea, Basov, Janecek, Palmer-Julson, et al., 1993). A subset of those samples, and samples from Sites 885 and 887, were analyzed for major and trace element concentrations in this post-cruise study. The results from the shipboard and shore-based laboratories are within analytical error of each other, so only the more complete shore-based data set is presented here (Table 1).

After shipboard examination of hand specimens and thin sections, 20 samples of representative diversity were selected for shore-based XRF analyses. Concentrations of 23 major and trace elements were measured at Washington State University on a wavelength-dispersive Rigaku 3370 automatic X-ray fluorescence spectrometer following the procedures of Hooper (1981). Each powdered sample was mixed with lithium tetraborate, fused, ground, and refused. Element concentrations were determined by comparing X-ray intensities from the unknowns with recommended values for eight international standards. Estimated precision and accuracy are generally better than 5% for major elements, and better than 10% for most trace elements, although precision can be less than 20% at concentrations below 50 ppm.

Seven of the samples that were analyzed by XRF were also selected for $^{40}Ar/^{39}Ar$ age determinations (Table 2). The least altered samples with the coarsest grained groundmass were usually preferred. All samples were crushed to 0.5–1-mm chips, ultrasonically washed in deionized water, and dried in a warm oven. Splits of approximately 1 g of the prepared chips were sealed in evacuated quartz tubes and irradiated in the Oregon State University (OSU) TRIGA reactor, where they received a neutron dose of approximately 0.7×10^{18} n/cm^2. The flux gradient and the efficiency of the conversion of ^{39}K to ^{39}Ar by neutron capture were monitored with samples of the biotite standard FCT-3 (27.7 ± 0.2 Ma; Hurford and Hammerschmidt, 1985). Further details of the sample preparation and irradiation procedures are given in Duncan (1991).

Argon extractions were performed at OSU by incremental heating in a glass extraction line using radio-frequency (RF) induction heating. Samples were held at each heating step for 30 min, and then analyzed with an AEI MS-10S mass spectrometer. Heating steps were set from RF power levels, determined from previous experience to divide total Ar into six approximately equal portions. After correction for background, mass fractionation, and isotopic interferences, the data were reduced to age spectra and $^{39}Ar/^{40}Ar$ vs. $^{36}Ar/^{40}Ar$ isotope correlation plots.

Two different methods were used to calculate plateau ages (Table 2) from heating steps that formed a contiguous sequence of at least three statistically indistinguishable (at 1σ) step ages. The first method weights each step age by the inverse of its variance to arrive at a weighted mean (Dalrymple et al., 1987). This mean emphasizes the more precisely determined step ages, and is the plateau age shown in the age spectra figures. The second method of calculating a mean weights each step by the $\%^{39}Ar$ released in that step. This method produces more conservative (larger) calculated standard errors than the first method, but otherwise there are no significant differences between the results from the two methods.

Isochron ages (Table 2) were determined from the $^{39}Ar/^{40}Ar$ vs. $^{36}Ar/^{40}Ar$ correlation plots, which allow independent determination of both the sample age and initial $^{40}Ar/^{36}Ar$ composition (McDougall

Table 1. Whole-rock major and trace element concentrations by XRF.

	Detroit Seamount														Chinook Trough	Patton-Murray seamount platform					
Hole:	883E					883F			884E						885A	887D					
Section:	20R-2	20R-3	21R-1	21R-5	21R-6	1R-3	2R-3	3R-1	2R-2	4R-4	6R-3	10R-4	10R-5	10R-6	8X-1	4R-4	7R-3	8R-2	10R-2	12R-1	13R-1
Interval (cm):	1–2	23–26	23–26	108–111	26–30	37–41	129–133	100–104	32–36	23–27	30–33	6–10	83–86	136–140	38–42	47–49	67–70	84–89	68–71	13–18	18–21
Oxide (wt%)																					
SiO_2	46.7	46.6	46.7	47.0	46.5	45.4	46.5	45.6	48.8	50.1	49.3	48.5	48.4	49.4	49.4	49.5	47.5	47.1	49.9	49.1	48.8
Al_2O_3	14.1	15.5	14.4	15.2	15.2	16.9	14.7	14.9	15.1	15.8	15.0	19.7	23.5	21.0	14.8	15.0	15.0	15.6	16.4	15.4	14.9
TiO_2	2.74	2.11	2.19	2.12	2.26	2.39	2.07	2.15	1.37	1.26	1.53	0.95	0.77	0.97	2.34	2.03	3.68	3.32	1.80	1.95	1.96
FeO*	13.7	11.4	10.4	10.8	10.8	12.8	11.1	13.7	10.8	9.0	11.1	7.6	5.6	7.0	12.2	10.1	13.2	13.1	9.1	11.2	11.5
MnO	0.22	0.12	0.15	0.17	0.19	0.18	0.12	0.15	0.18	0.16	0.16	0.11	0.10	0.11	0.20	0.22	0.16	0.16	0.12	0.19	0.19
CaO	11.4	12.6	12.8	11.7	11.4	12.1	12.7	11.8	11.6	13.2	12.1	13.4	14.3	14.0	11.3	11.9	8.0	8.3	11.9	11.6	11.1
MgO	6.01	4.70	6.11	6.96	7.09	1.77	5.95	5.13	8.82	6.75	7.11	6.99	4.60	5.02	5.35	6.43	5.66	6.34	5.44	5.25	6.41
K_2O	0.39	1.24	1.06	0.63	0.53	1.46	1.09	1.20	0.10	0.61	0.13	0.11	0.35	0.25	0.54	0.52	0.85	0.84	0.53	0.63	0.70
Na_2O	3.04	2.99	2.85	3.04	3.07	3.37	2.81	2.86	2.42	2.74	2.84	2.28	2.14	2.32	2.83	3.21	3.69	3.27	3.28	2.85	2.43
P_2O_5	0.32	0.31	0.24	0.23	0.25	0.45	0.23	0.30	0.11	0.09	0.11	0.08	0.06	0.08	0.20	0.30	0.55	0.45	0.19	0.43	0.18
Total	98.56	97.61	96.87	97.90	97.28	96.88	97.25	97.77	99.37	99.72	99.39	99.72	99.77	100.06	99.13	99.13	98.30	98.38	98.67	98.59	98.09
Trace element (ppm)																					
Ni		76	63	69	74	61	134	49	79	94	72	85	47	72	42	64	31	45	53	33	31
Cr		150	158	153	159	151	146	147	302	198	271	246	214	245	196	219	74	85	131	118	120
Sc		41	44	40	43	41	34	37	49	48	47	35	28	34	45	31	30	32	38	45	44
V		297	291	325	335	325	288	348	297	313	355	201	165	236	414	257	316	278	248	301	301
Ba		46	19	26	29	96	44	54	4	0	0	4	0	0	0	161	131	125	13	6	0
Rb		71	51	4	5	21	53	50	1	14	2	1	7	6	13	7	14	9	12	12	8
Sr		234	217	213	214	294	215	228	123	113	128	149	160	159	145	427	280	281	208	194	163
Zr		135	137	132	141	147	133	137	81	67	84	60	50	60	144	115	272	237	118	127	125
Y		33	35	33	33	36	33	33	31	31	33	21	16	21	43	24	46	38	31	36	37
Nb		10	12	10	10	11	11	11	4	3	5	2	2	3	7	22	35	30	7	10	9
Ga		19	26	21	22	21	21	21	15	16	20	16	18	14	25	19	27	29	20	22	17
Cu		88	128	103	100	100	129	89	140	106	180	112	101	109	52	75	34	39	76	79	72
Zn		180	103	93	92	135	102	151	74	73	100	59	51	52	120	100	130	118	90	102	97

Notes: Sample 145-883E-20R-2 is an average of 4 glass analyses by electron microprobe at OSU; FeO* is total Fe as FeO.

Table 2. $^{40}Ar/^{39}Ar$ plateau and isochron ages for basalts from Leg 145.

Core, section, interval (cm)	Plateau age ± 1σ (Ma) Weighted by $1/\sigma^2$	Weighted by % ^{39}Ar	Isochron age ± 1σ (Ma)	Integrated age (Ma)	^{39}Ar (% of total)	N	SUMS (N - 2)	$^{40}Ar/^{36}Ar$ intercept
145-883F-								
1R-3, 37–41	No plateau developed			(50.4)				
2R-3, 129–133	No plateau developed			(52.6)				
145-884E-								
10R-4, 6–10, pl	No plateau developed			(128.1)				
10R-4, 6–10, np	81.2 ± 1.3	80.8 ± 2.6	80.0 ± 0.9	77.8	85.1	5	0.1	294.6 ± 4.0
10R-6, 136–140	No plateau developed			(47.5)				
145-885A-								
8X-1, 38–42	80.0 ± 1.0	80.6 ± 1.2	79.3 ± 0.8	80.6	100.0	5	0.1	301.0 ± 3.3
145-887D-								
4R-4, 47–49	17.1 ± 0.3	17.0 ± 0.5	16.8 ± 0.5	17.0	100.0	6	1.7	295.4 ± 1.4
7R-3, 67–70	27.3 ± 0.3	27.4 ± 0.3	27.5 ± 0.4	27.4	100.0	5	3.0	292.7 ± 2.1

Notes: The pl and np suffixes for Sample 145-884E-10R-4, 6–10 cm, denote plagioclase-megacryst separate and plagioclase-megacryst-free separates, respectively. Integrated ages given in parentheses are unreliable and are not crystallization ages.

Table 3. Representative analyses of minerals in Sample 145-884E-10R-4, 0–4 cm.

					Rim	Core
	Olivine	Clinopyroxene			Plagioclase	
Oxide (wt%)						
SiO_2	39.60	52.60	49.87	49.29	55.52	49.53
Al_2O_3	0.04	2.11	1.85	3.33	27.33	31.66
TiO_2	0	0.63	1.14	1.64		
FeO*	14.48	8.42	19.02	13.90	0.84	0.52
MnO	0.14	0.21	0.57	0.38		
CaO	0.38	19.89	17.71	18.66	9.94	14.96
MgO	45.32	16.15	9.83	12.65	0.12	0.27
Na_2O		0.26	0.38	0.46	5.81	2.96
K_2O					0.08	0.03
NiO	0.16					
Cr_2O_3		0.08	0	0.01		
Total	100.12	100.35	100.37	100.32	99.64	99.93

Notes: Olivine = average of four analyses of a single phenocryst; concentrations are by electron microprobe at Oregon State University; FeO* = total Fe as FeO.

and Harrison, 1988). Only those steps that had concordant ages in the plateau plots were used for the isochron. The goodness-of-fit parameter SUMS has a χ^2-distribution with (N – 2) degrees of freedom (York, 1969), with N being the number of steps used for the isochron regression. Experiments that yield an acceptable goodness-of-fit, a $^{40}Ar/^{36}Ar$ intercept near the atmospheric value (295.5), and relatively concordant isochron and plateau ages are likely to have determined reliable crystallization ages (Lanphere and Dalrymple, 1978).

Apparent Ca/K was calculated for each heating step using the relationship $Ca/K = 1.852 \times {}^{37}Ar/{}^{39}Ar$ (Fleck et al., 1977; Walker and McDougall, 1982).

Microprobe analyses were done on a four-spectrometer Cameca SX-50 at OSU using natural mineral phases and basalt glass from the Smithsonian reference collection as standards. Software provided with the microprobe corrected measured concentrations for atomic number, absorption, and fluorescence effects. Glass in Sample 145-883E-20R-2, 1–2 cm, (Table 1) was analyzed with 15-kV accelerating voltage, 30-nA beam current, and 10-s counting times, except Ti and Al were counted for 20 s. Precision based upon multiple analyses of the Makaopuhi basalt glass is reported in Forsythe and Fisk (1994). Conditions for the plagioclase analyses (Tables 3 and 4) were 15-kV accelerating voltage, 30-nA beam current, and 10-s counting times. Conditions for the clinopyroxene and olivine analyses (Tables 3 and 4) were 15-kV accelerating voltage, 50-nA beam current, and 10-s counting times, except Ti was counted for 20 s. Na was analyzed first in all procedures, and showed no evidence for loss under these conditions.

RESULTS

Detroit Seamount

Whole-rock Chemistry

Site 883

All seven of the Site 883 samples analyzed by XRF are chemically similar to each other (Table 1), and show no systematic variation with stratigraphic position. Their MgO contents range from 2 to 7 wt% (Fig. 2), although the sample with the lowest MgO also has the lowest SiO_2 (Table 1), and there is no correlation between MgO content and Ni or Cr content. Incompatible element concentrations increase slightly with decreasing MgO, except that those elements most susceptible to alteration (e.g., K, Rb, Ba) do not show a correlation with MgO. Incompatible element ratios are essentially constant (except for those elements susceptible to alteration). What little variation there is in the Site 883 samples that is not due to alteration can be accounted for by minor amounts of fractional crystallization.

The two samples with the highest MgO contents have one-half of the K_2O and an order of magnitude lower Rb than the other samples, and may be the least altered samples recovered at the site. Aboard ship the area of the core around these two samples appeared fresher (blacker) than the rest of the core. Samples from deeper in the hole than these two samples were not analyzed on shore, but shipboard trace element analyses suggest that they are similar to samples from the upper part of the section.

The highly altered condition of the samples makes it difficult to determine whether their original igneous compositions were alkalic or tholeiitic. The two samples thought to be the least altered are the lowest in $Na_2O + K_2O$, but still plot above the silica saturation line in SiO_2 vs. $Na_2O + K_2O$ space. However, all of the samples may be too altered to be classified using the alkali elements. TiO_2 contents in the samples are between 2.1 and 2.4 wt%, which when compared to Hawaiian alkalic and tholeiitic basalts is not diagnostic of either. The same is true for other incompatible elements. Thus the samples may be transitional. The chemistry of the Site 883 basalts is quite similar to that of the DSDP Site 192 (Meiji Seamount) basalt, which was tentatively classified based upon mineralogy as an alkali basalt (Stewart et al., 1973), but later analyses of glass and pyroxene in the sample suggested that it may be tholeiitic (Dalrymple et al., 1980). The composition of the Site 883 basalts is equally as ambiguous.

Many of the pillow margins recovered at Site 883 contained fresh glass. Microprobe analyses of the glass (Table 1) yielded data similar to the whole-rock XRF analyses, with the exception of K_2O, which is much lower in the glass. This may represent the true K_2O content of the Site 883 basalts prior to alteration, in which case the Site 883 basalts

are less alkalic than indicated by the whole-rock data, but would still be classified as alkalic basalts based upon SiO_2 vs. total alkalis.

Site 884

The six samples from Site 884 analyzed by XRF (Table 1) range from 4.6 to 8.8 wt% MgO (Fig. 2). Their low alkali contents suggest that they are tholeiitic (Table 1). Four of the samples contained plagioclase megacrysts (Rea, Basov, Janecek, Palmer-Julson, et al., 1993), which explains their higher Al_2O_3 and CaO contents and consequently lower MgO, TiO_2, and FeO* contents. The small chemical differences between the samples that are not due to alteration or the effects of the plagioclase megacrysts can be accounted for by minor amounts of fractional crystallization.

Even when the effects of the plagioclase megacrysts are considered, all of the Site 884 samples have unusually low incompatible trace element concentrations when compared with typical ocean island tholeiites. Their moderate MgO and Ni contents indicate that they are not of exceptionally primitive composition, so their low incompatible element concentrations must be due to large extents of melting, or melting of an unusually depleted source. Tholeiitic basalts with such low incompatible element concentrations (TiO_2 <1.5, Sr <200, Zr <100) have not been reported from the Hawaiian Islands, but do occur at other ocean islands (e.g., Galapagos: Geist et al., 1986; White et al., 1993; Nauru: Castillo et al., 1986; Réunion/Kerguelen: Weis et al., 1992). Site 884 was located deep on the flank of Detroit Seamount, and may represent an early phase of volcanism that is not usually sampled by dredges or exposed on islands.

Mineral Chemistry

Site 884

A few representative microprobe analyses of phenocrysts in Sample 145-884E-10R-4, 0–4 cm, are given in Table 3. The clinopyroxene compositions are compatible with the tholeiitic nature of the basalts: TiO_2 and Al_2O_3 contents are higher than in clinopyroxenes from mid-ocean ridge tholeiites, but similar to clinopyroxenes in tholeiites from Suiko Seamount (Clague et al., 1980).

$^{40}Ar/^{39}Ar$ Geochronology

Site 883

All of the samples from Site 883 are fine grained and have highly altered groundmass; however, two of the coarsest grained and least altered were selected for $^{40}Ar/^{39}Ar$ dating. Sample 145-883F-1R-3, 37–41 cm, is a highly plagioclase-olivine-microphyric basalt from a pillow interior. Sample 145-883F-2R-3, 129–133 cm, is a moderately plagioclase-microphyric basalt from a pillow interior. Neither of these samples yielded a concordant plateau age (Fig. 3), and could not be fit with a statistically significant isochron. Both samples show a decrease in apparent age with increasing temperature steps, which is characteristic of samples that have experienced ^{39}Ar recoil from relatively K-rich to K-poor sites during neutron irradiation. It also appears that these samples have lost radiogenic ^{40}Ar from low-temperature sites. In this case the only age estimates possible are calculated by recombining the Ar compositions from all temperature steps (Integrated ages 50 to 53 Ma in Table 2). In view of the likelihood of radiogenic ^{40}Ar loss, we consider these as *minimum* age estimates only. The extensive alteration and fine-grained nature of the samples recovered at Site 883 make them poorly suited to $^{40}Ar/^{39}Ar$ analysis, and further dating of samples from this site was not attempted.

Site 884

Sample 145-884E-10R-4, 6–10 cm, is a highly plagioclase-olivine-clinopyroxene-phyric basalt containing plagioclase megacrysts. This sample was hand-picked into a plagioclase component and a plagioclase-free component and was run as two separate samples. The plagioclase separate did not yield a reliable isochron or concordant plateau age (Fig. 4). The erratic and high apparent ages of most of the heating steps are consistent with excess ^{40}Ar in the megacrysts due to incomplete equilibration with atmospheric ^{40}Ar upon eruption. The integrated age of this sample, which does not represent a true crystallization age, is 128.1 Ma (Table 2). The plagioclase-free component of this same sample, however, yielded a good plateau age and isochron (Fig. 5). The calculated plateau age is 81.2 ± 1.3 Ma, and the calculated isochron age is 80.0 ± 0.9 Ma (Table 2), which are concordant. Isotopic data for the five steps that define the plateau produced an excellent isochron fit, with an initial $^{40}Ar/^{36}Ar$ of atmospheric composition. Hence, we conclude that the tholeiitic portion of Detroit Seamount was constructed at 81 Ma. The phases outgassing during the first five temperature steps have similar Ca/K ratios (Fig. 5C), appropriate to fine-grained matrix. The highest temperature step,

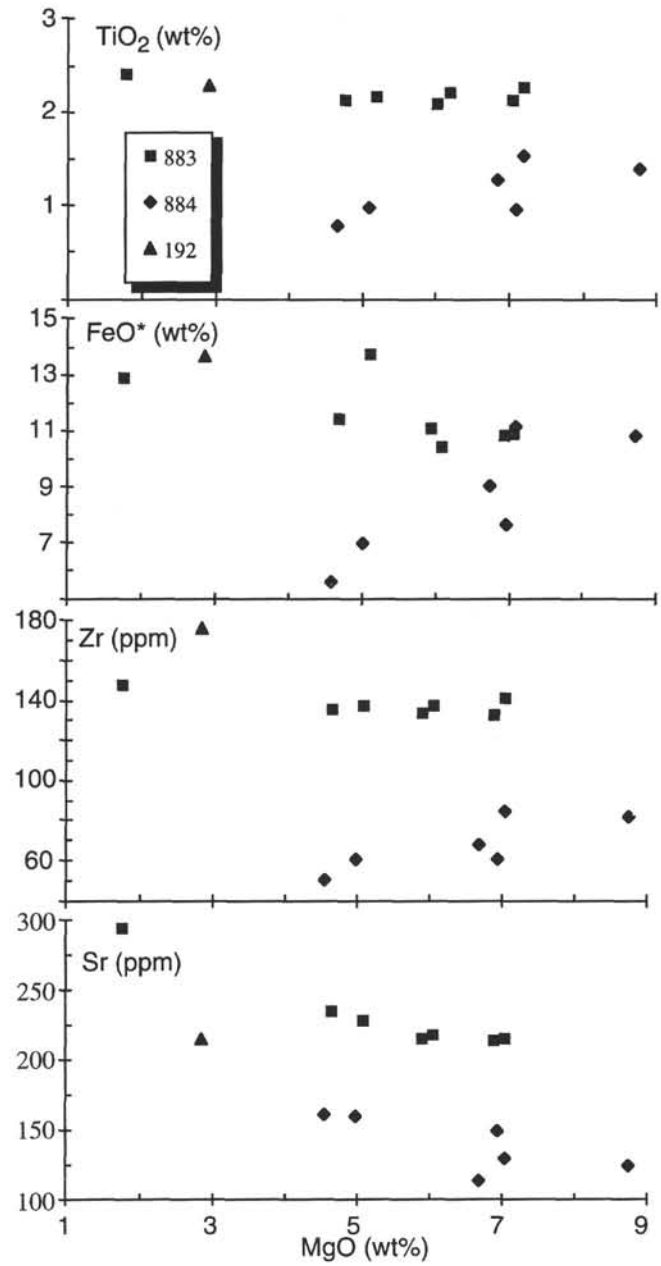

Figure 2. MgO vs. TiO_2, FeO*, Zr, and Sr for samples from Detroit Seamount (Sites 883 and 884) and Meiji Seamount (DSDP Site 192).

Table 4. Representative analyses of minerals in samples from Site 887.

Clinopyroxene							
Sample:	887D-4R-4, 49–50 cm	887D-7R-3, 67–70 cm			887D-10R-2, 68–71 cm		
Description:	Gm	Core	Rim	Core	w/mega	Gm	Gm
Oxide (wt%)							
SiO_2	47.13	44.51	48.70	46.36	47.01	48.88	52.69
Al_2O_3	5.17	7.25	3.64	5.44	6.02	4.97	2.14
TiO_2	1.95	4.10	1.70	3.21	2.59	1.74	0.58
FeO*	8.35	10.92	13.85	11.23	11.82	8.83	6.14
MnO	0.16	0.15	0.33	0.24	0.21	0.18	0.15
CaO	20.58	20.84	20.48	21.16	19.91	20.96	21.17
MgO	13.86	11.43	10.68	11.52	12.17	13.96	16.84
Na_2O	0.38	0.43	0.43	0.45	0.42	0.34	0.23
Cr_2O_3	0.27	0.02	0	0	0	0.03	0.12
Total	97.85	99.65	99.81	99.61	100.15	99.89	100.06

Plagioclase				
Sample:	887D-4R-4, 49–50 cm		887D-10R-2, 68–71 cm	
Description:	Rim	Core	Gm	Mega
Oxide (wt%)				
SiO_2	61.46	50.73	50.86	45.01
Al_2O_3	23.26	29.91	30.94	35.35
FeO*	0.34	0.58	0.61	0.20
CaO	4.49	13.01	14.03	18.08
MgO	0.02	0.14	0.16	0.17
Na_2O	8.39	3.93	3.43	1.16
K_2O	0.81	0.19	0.06	0.04
Total	98.77	98.49	100.09	100.01

Notes: Concentrations are by electron microprobe at Oregon State University; FeO* is total Fe as FeO. Gm = groundmass crystal, Core = core of phenocryst, Rim = rim of phenocryst, w/mega = in glomerocryst with plagioclase megacryst, Mega = megacryst.

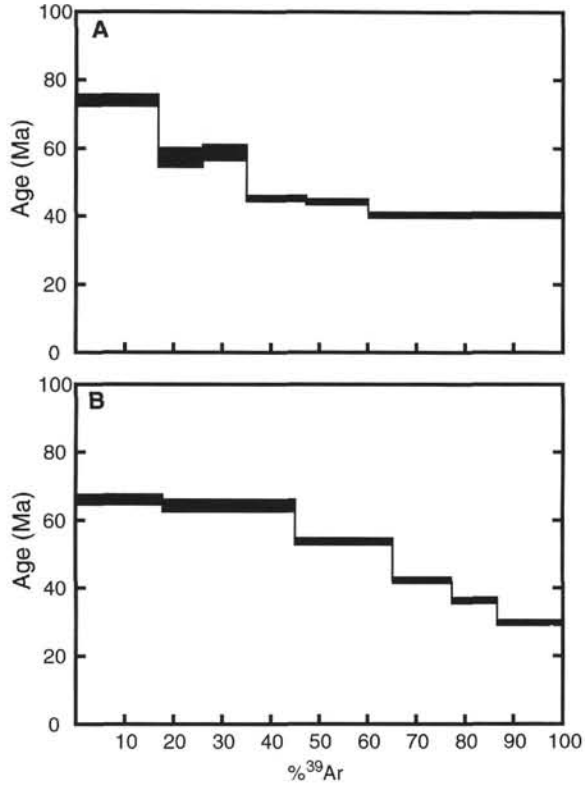

Figure 3. Apparent age spectrum (plateau) diagrams. **A.** Sample 145-883F-1R-3, 37–41 cm. **B.** Sample 145-883F-2R-3, 129–133 cm. Heights of the black boxes indicate the analytical standard error (±1 σ) around each calculated step age.

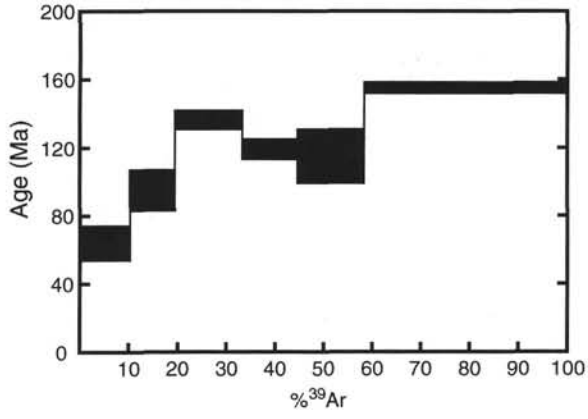

Figure 4. Apparent age spectrum (plateau) diagram for Sample 145-884E-10R-4, 6–10 cm (plagioclase separate). Details as in Figure 3.

which yielded a younger age than the plateau, reflecting radiogenic ^{40}Ar loss, produced a Ca/K appropriate to plagioclase (200–800; Table 3).

Sample 145-884E-10R-6, 136–140 cm, is a highly plagioclase-phyric basalt from a pillow interior. This sample did not yield a reliable isochron or concordant plateau age (Fig. 6), and appears to have lost radiogenic ^{40}Ar during alteration. The small age plateau at approximately 80 Ma may be fortuitous in its similarity to the crystallization age of Sample 145-884E-10R-4, 6–10 cm, or it may represent the crystallization age.

Chinook Trough (Site 885/886)

Whole-rock Chemistry

One of the aphyric basalt cobbles from Site 885 (Sample 145-885A-8X-1, 38–42 cm) was selected for XRF analysis (Table 1). The

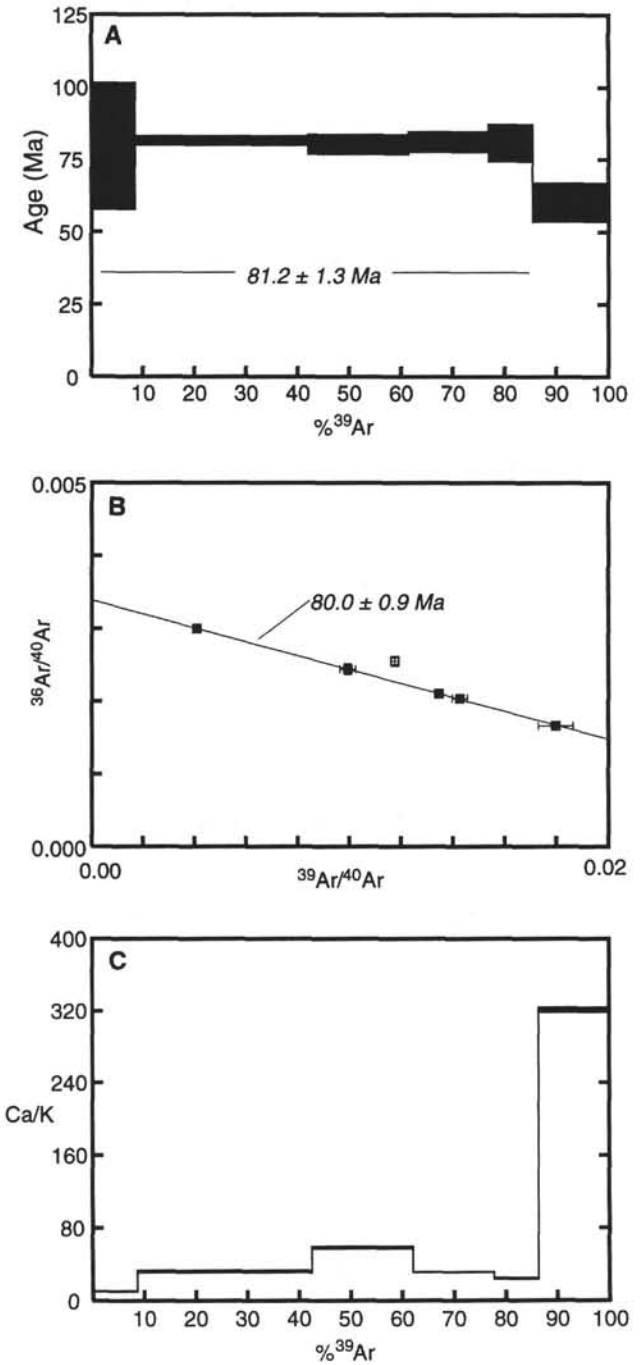

Figure 5. Radiometric dating results for Sample 145-884E-10R-4, 6–10 cm, (plagioclase-free). **A.** Apparent age spectrum (plateau) diagram. **B.** $^{39}Ar/^{40}Ar$ vs. $^{36}Ar/^{40}Ar$ isochron diagram with a point for each heating step shown in (A). **C.** Apparent Ca/K release diagram. Heights of the black boxes in the gas release plots (A and C) indicate the analytical standard error (±1 σ) around each calculated step age or Ca/K. A plateau age (Table 2) was determined from the weighted mean of contiguous, concordant gas increment steps. The isochron age was determined from the best-fitting line to collinear gas increment compositions (filled squares), after York (1969). The Ca/K compositions reflect the minerals outgassing as a function of temperature.

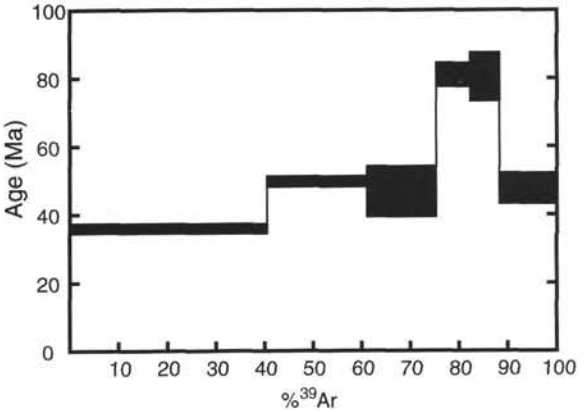

Figure 6. Apparent age spectrum (plateau) diagram for Sample 145-884E-10R-6, 136–140 cm. Details as in Figure 3.

basalt has 5.4 wt% MgO (Fig. 7) and 49.4 wt% SiO_2. It plots as a subalkaline basalt, but the alkali and alkali earth element concentrations in this sample are suspect because of alteration. High Y (and therefore low Zr/Y and Nb/Y) is consistent with mid-ocean ridge tholeiites.

$^{40}Ar/^{39}Ar$ Geochronology

The same aphyric basalt cobble that was selected for XRF was also sampled for $^{40}Ar/^{39}Ar$ age dating. The sample yielded a plateau age of 80.0 ± 1.0 Ma, and an isochron age of 79.3 ± 0.8 Ma (Fig. 8 and Table 2). The isochron age is statistically significant, and the $^{40}Ar/^{36}Ar$ intercept is only slightly above the atmospheric value. Hence, we conclude that 80 Ma is a reliable crystallization age for this basalt. This age is younger than the Early? Cretaceous age of seafloor in the area predicted from analysis of marine magnetic anomalies (Rea and Dixon, 1983), but is consistent with the observation that the basalt was encountered after drilling only 66 m of sediment instead of the 150 m of sediment expected from interpretation of seismic reflections records. Also, drilling did not penetrate the Lower Cretaceous carbonates that are thought to underlie all of the North Pacific (Rea, Basov, Janecek, Palmer-Julson, et al., 1993). The high stratigraphic position and young age of the basalt, therefore, suggest that it is not true basement, but represents a volcanic rejuvenation of the area associated with the Late Cretaceous plate reorganization at approximately 82 Ma (Rea and Dixon, 1983; Rea, Basov, Janecek, Palmer-Julson, et al., 1993). Volcanism associated with the Chinook Trough spreading center apparently affected a wider area of the north-central Pacific than was previously thought.

Patton-Murray Seamount Platform

Whole-rock Chemistry

Six representative basalts from a range of depths in Hole 887D were chosen for XRF analysis. Their narrow ranges in MgO and SiO_2 contents (5.2 to 6.4 wt% and 47.1 to 49.5 wt%, respectively; Table 1 and Fig. 7) contrast with their much wider relative ranges of many other elements (Table 1). Nb contents vary by a factor of 5 (7 to 35 ppm), whereas most other incompatible elements vary by a factor of 2 or so (e.g., Sr = 163–427 ppm; Zr = 115–272 ppm; Y = 24–46 ppm). With the exception of Ba, alteration does not appear to be controlling these variations. Nor can simple fractional crystallization explain these variations.

Mineral Chemistry

Representative electron microprobe analyses of clinopyroxene and plagioclase in the Site 887 basalts are given in Table 4. The high TiO_2 and Al_2O_3 in clinopyroxene in Sample 145-887D-7R-3, 67–70

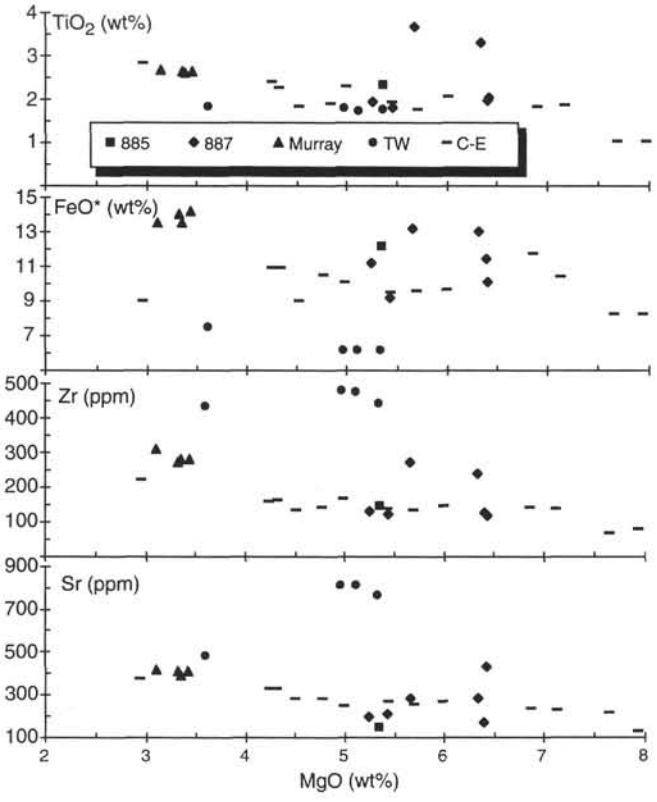

Figure 7. MgO vs. TiO_2, FeO*, Zr, and Sr for samples from Chinook Trough (Site 885) and Patton-Murray seamount platform (Site 887). Shown for comparison are data from other seamounts in the northeast Pacific. Murray = Murray Seamount (data from Dalrymple et al., 1987), TW = Tuzo Wilson Seamounts (data from Allan et al., 1993), and C-E = Cobb-Eickelberg Seamounts (data from Desonie and Duncan, 1990). Murray Seamount is 40 km from Site 887. Locations of Cobb-Eickelberg and Tuzo Wilson Seamounts are shown in Figure 1.

cm, reflects the strongly alkalic character of the middle group of basalts. Clinopyroxene in Sample 145-887D-10R-2, 68–71 cm, from the lower group of basalts is much lower in TiO_2 and Al_2O_3, with the exception of a clinopyroxene that is in a glomerocryst with a plagioclase megacryst. Plagioclase analyses from that same sample show the large contrast between the megacrysts, which are An_{90}, and groundmass phenocrysts of plagioclase (Table 4).

$^{40}Ar/^{39}Ar$ Geochronology

Two samples were selected from Site 887 for $^{40}Ar/^{39}Ar$ age determinations. Sample 145-887D-4R-4, 47–49 cm, is a highly plagioclase-clinopyroxene-phyric basalt from a flow interior at 291.01 meters below sea floor (mbsf) (Fig. 9). The sample yielded a good age plateau and isochron (Fig. 10). The calculated plateau age (using all heating steps) is 17.1 ± 0.3 Ma, and the calculated isochron age is concordant at 16.8 ± 0.5 Ma (Table 2). The isochron fit is statistically significant, and the $^{40}Ar/^{36}Ar$ intercept is atmospheric composition (Table 2).

Sample 145-887D-7R-3, 67–70 cm, is a highly clinopyroxene-plagioclase-phyric basalt from a flow interior at 309.33 mbsf (Fig. 9). The sample yielded a good age plateau and isochron (Fig. 11). The weighted mean plateau age is 27.3 ± 0.3 Ma, and the calculated isochron age is concordant at 27.5 ± 0.4 Ma (Table 2). The excellent fits of the isochrons and the initial $^{40}Ar/^{36}Ar$ of atmospheric composition in both Site 887 samples (Table 2) lead us to conclude that these represent crystallization ages. The age of the lower basalt is within analytical error of the 27.6 ± 0.2 Ma $^{40}Ar/^{39}Ar$ age reported by Dalrymple et al. (1987) for basalt dredged from Murray Seamount, 40 km from Site 887.

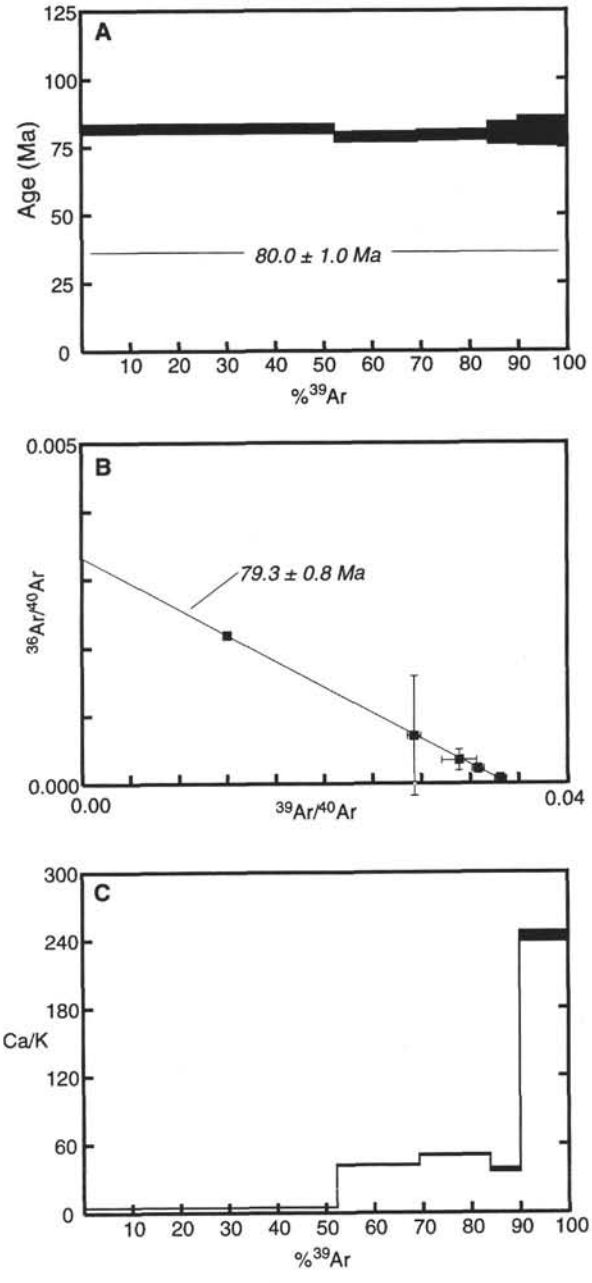

Figure 8. Radiometric dating results for Sample 145-885A-8X-1, 38–42 cm. **A.** Apparent age spectrum (plateau) diagram. **B.** $^{39}Ar/^{40}Ar$ vs. $^{36}Ar/^{40}Ar$ isochron diagram. **C.** Apparent Ca/K release diagram. Details as in Figure 5.

DISCUSSION

Detroit Seamount

When the 81 Ma age of Detroit Seamount and its distance from the island of Hawaii (measured along the seamount chain) are compared to data for other volcanoes in the Hawaiian-Emperor volcanic chain (Clague and Dalrymple, 1987), the Detroit Seamount sample appears to be too old (Fig. 12). Extrapolation of distance vs. age data from the <65 Ma Hawaiian-Emperor Seamounts (Suiko and younger) predicts that Detroit Seamount should be 65 to 75 m.y. old. A similar result is obtained from a model for Pacific plate motion in the hotspot reference frame based on a best fit to radiometric ages of Pacific island and seamount lineaments (Duncan and Clague, 1985). Part of this age discrepancy could be explained if the Detroit Seamount sample is from early in the history of the volcano, as its tholeiitic composition

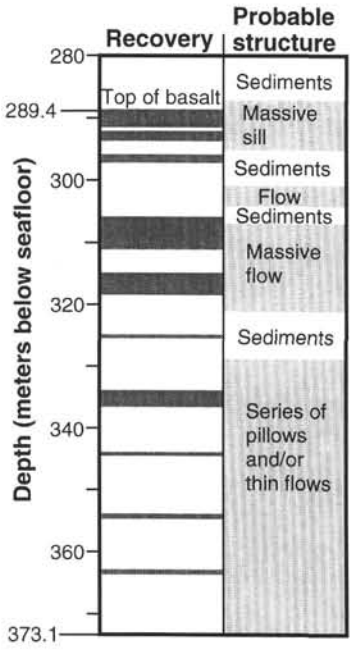

Group	Samples	Age (Ma)	MgO (wt%)	TiO_2 (wt%)	Sr/Y	Zr/Nb
Upper	4R-4, 47–49 cm	17	6.4	2.0	18	5
Middle	7R-3, 67–70 cm	27	5.7	3.7	6	8
	8R-2, 84–89 cm		6.3	3.3	7	8
	10R-2, 68–71 cm		5.4	1.8	7	17
Lower	12R-1, 13–18 cm	?	5.3	1.9	5	13
	13R-1, 18–21 cm		6.4	2.0	4	14

Figure 9. Stratigraphy for the basement portion of Hole 887D interpreted from downhole logging data and core recovery data (Rea, Basov, Janecek, Palmer-Julson, et al., 1993). Radiometric ages for the middle and upper groups of basalts are shown. Some geochemical characteristics of all three basalt groups are also shown.

suggests. But typical estimates of the lifespan of a Hawaiian volcano are less than 2 m.y., unless an alkalic rejuvenated stage occurs and extends the lifespan of the volcano to as much as 4 m.y. (Clague and Dalrymple, 1987). So even if the Detroit Seamount tholeiite is from early in the history of the volcano, it appears that previous plate motion models overestimate the velocity of the Pacific plate relative to the Hawaiian hotspot prior to approximately 65 Ma. The velocity of the Pacific plate must have increased sometime between when Detroit Seamount formed at 81 Ma and when Suiko Seamount formed at 65 Ma. Paleomagnetic (Sager and Pringle, 1988) and geochronological (Duncan and Clague, 1985) data from other Pacific seamount chains also suggest at least one change in Pacific plate motion between 81 and 65 Ma.

Patton-Murray Seamount Platform

The 17 Ma age of the uppermost Site 887 basalt has interesting implications for its mode of emplacement. The extraordinarily complete paleomagnetic record of the sediments at Site 887 is continuous down to the top of Chron 5eN (18.3 Ma) at 272 mbsf (Rea, Basov, Janecek, Palmer-Julson, et al., 1993), which is still 19 m above the basalt. The sedimentation rate in that part of the section (5 m/m.y.) suggests that those 19 m represent another 3–4 m.y. of time. Thus the uppermost basalt would be expected to be approximately 21–22 m.y. old if it were erupted onto the seafloor. Paleontological evidence also suggests that the sediments directly overlying the basalt are early Miocene in age (Rea, Basov, Janecek, Palmer-Julson, et al., 1993). Apparently the uppermost basalt is a sill that intruded sediments that were 4–5 m.y. old at the time. The resistivity and bulk density logs show that this sill is 6–7 m thick (Fig. 9), 4 m of which was recovered (Rea, Basov, Janecek, Palmer-Julson, et al., 1993). Such a massive flow should not have had any trouble intruding the soft sediments. Unfortunately, the contact between the sill and the overlying sediments was not recovered, so its nature could not be determined.

A small amount of sediment recovered between the uppermost basalt and the middle group of basalts (Fig. 9) contained Oligocene to early Miocene radiolarians, an Oligocene calcareous nannofossil assemblage, and late Oligocene benthic foraminifers (Rea, Basov, Janecek, Palmer-Julson, et al., 1993). These ages fit between the 17 and 27 Ma ages of the basalts above and below the recovered sediment.

The 10-m.y. age difference between the two dated Site 887 samples is unusual, but is not unprecedented in a single seamount platform (Rurutu, Austral Islands: Duncan and McDougall, 1976; Kodiak-Bowie seamount chain: Chapman et al., 1987; Christmas Island: T. Falloon et al., unpublished data, 1994). Our knowledge of the lifespan of ocean island volcanoes and seamount platforms may be biased by the fact that nearly all of the samples from these locations are taken from the volcanic summits that can be dredged or can be sampled where they project above sea level.

The whole-rock geochemistry of the Site 887 samples supports the complex history of the seamount platform suggested by the age data. The samples can be divided into three groups (Fig. 9) an alkalic to transitional group represented by Sample 145-887D-4R-4, 47–49 cm, and characterized by high Sr/Y and low Zr/Nb; a strongly alkalic group represented by Samples 145-887D-7R-3, 67–70 cm, and 145-887D-8R-2, 84–89 cm, and characterized by high TiO_2 and low Sr/Y and Zr/Nb; and a tholeiitic to transitional group represented by Samples 145-887D-10R-2, 68–71 cm, 145-887D-12R-1, 13–18 cm, and 145-887D-13R-1, 18–21 cm, and characterized by low Sr/Y and high Zr/Nb. These three groups also occur in stratigraphic order (Fig. 9), with the alkalic to transitional group at the top (dated at 17 Ma), the strongly alkalic group in the middle (dated at 27 Ma), and the tholeiitic to transitional group at the bottom (undated). The volcanic stratigraphy of the hole can be assembled from the geochemical data, the recovered cores, and the downhole logging data (Rea, Basov, Janecek, Palmer-Julson, et al., 1993). Resistivity and bulk density logs and hole diameter data from the caliper tool show an upper massive sill, two massive flows in the middle, and a lower series of thin flows or pillows (Fig. 9). These three flow groups coincide with the geochemical groups, and can be shown on the logs to be separated by several meters of sediments.

Although Site 887 is the only place where one of the northeast Pacific seamounts has been drilled, several of these seamounts have been dredged. Dalrymple et al. (1987) reported analyses of samples from the Gulf of Alaska seamounts, including four samples dredged from Murray Seamount, 40 km from Site 887. The Murray samples are more evolved than anything recovered at Site 887 (Fig. 7), but the Sr/Y

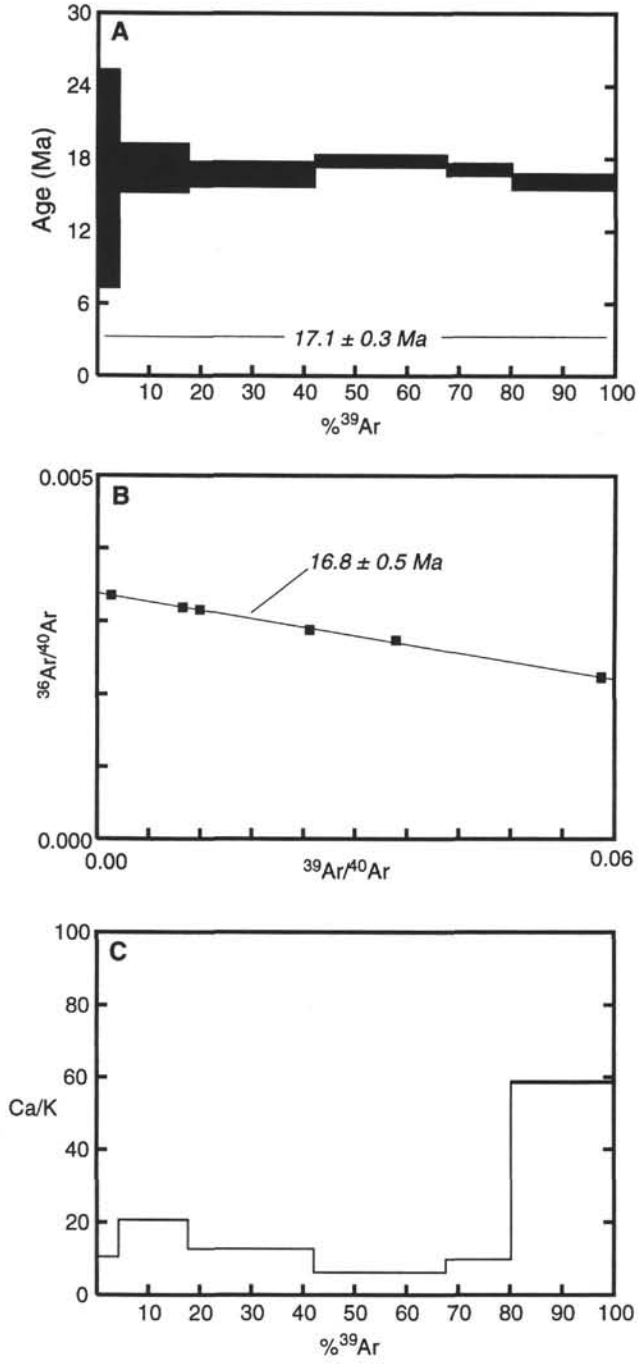

Figure 10. Radiometric dating results for Sample 145-887D-4R-4, 47–39 cm. **A.** Apparent age spectrum (plateau) diagram. **B.** $^{39}Ar/^{40}Ar$ vs. $^{36}Ar/^{40}Ar$ isochron diagram. **C.** Apparent Ca/K release diagram. Details as in Figure 5.

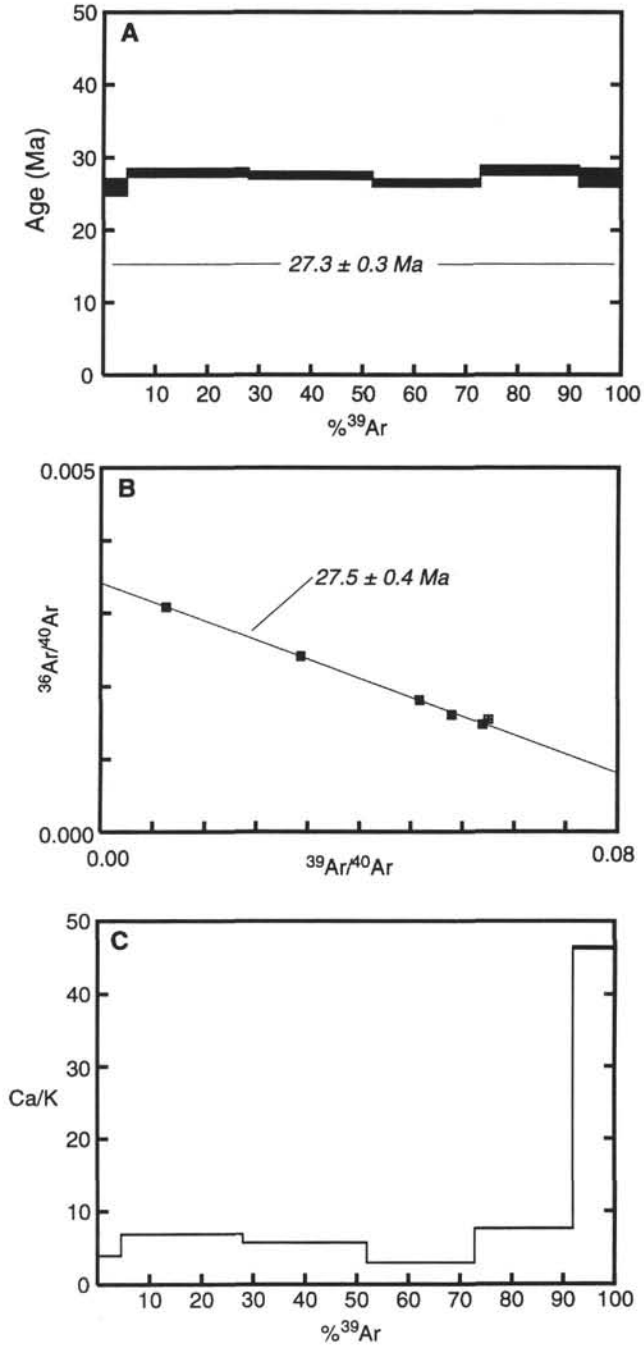

Figure 11. Radiometric dating results for Sample 145-887D-7R-3, 67–70 cm. **A.** Apparent age spectrum (plateau) diagram. **B.** $^{39}Ar/^{40}Ar$ vs. $^{36}Ar/^{40}Ar$ isochron diagram. **C.** Apparent Ca/K release diagram. Details as in Figure 5.

(6–7) and Zr/Nb (7–10) of the dredged samples are similar to the middle group of basalts recovered at Site 887. Dalrymple et al. (1987) obtained a radiometric age of 27 Ma for a Murray sample, which matches with the age of the middle group of basalts (Fig. 9). Samples dredged from the Tuzo Wilson Seamounts (Fig. 1; Allan et al., 1993) have much higher trace element concentrations at a given MgO content, and are compositionally distinct from the Site 887 basalts (Fig. 7).

The Cobb-Eickelberg seamount chain (Fig. 1) extends northwestward from the Juan de Fuca Ridge and formed at the Cobb hotspot from 9 Ma to the present (Desonie and Duncan, 1990). The Patton-Murray seamount platform lies along the northwestward extension of the Cobb-Eickelberg trend in the direction of Pacific plate motion, and could also have formed above the Cobb hotspot (Duncan and Clague, 1985). However, backtracking of Patton-Murray Seamounts to 27 Ma using the Pacific plate motion models of Duncan and Clague (1985) and Pollitz (1988) places them 150–250 km west of the Cobb hotspot. For the Patton-Murray Seamounts to be related to the Cobb hotspot, the 27 Ma basalts would have to represent a volcanic rejuvenescence of the seamounts. The higher alkali and TiO_2 contents of the middle and upper groups of Site 887 basalts and the basalts dredged from Murray Seamount (Dalrymple et al., 1987) are consistent with their eruption during a low-degree-partial-melt, rejuvenescent phase

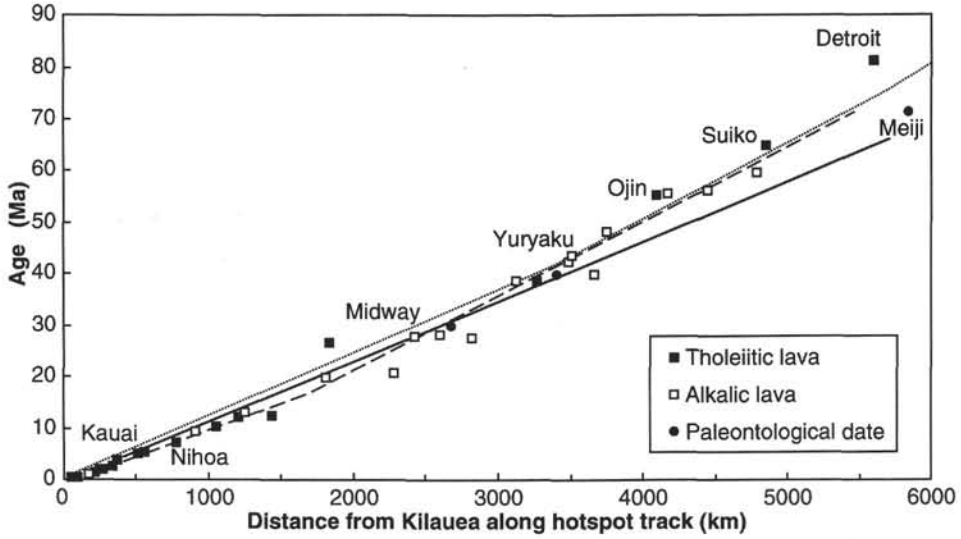

Figure 12. Distance (measured along seamount chain) from Kilauea vs. age for islands and seamounts in the Hawaiian-Emperor chain (modified from Clague and Dalrymple, 1987). Solid line is a least-squares cubic fit to all of the data, regardless of stage of volcano-building. Dashed line is a two-segment fit. Dotted line is a four-stage rotation sequence (from Duncan and Clague, 1985) for the Pacific plate over hotspots, best fit to radiometric age determinations of Pacific island and seamount lineaments. "Detroit" data point is from this study.

of volcanism downstream from the Cobb hotspot. Late-stage volcanic phases are a common feature of other hotspot lineaments (e.g., Hawaiian, Society, and Réunion hotspots).

The lower group of basalts from Site 887 is chemically indistinguishable from the Cobb-Eickelberg basalts (Fig. 7). Trace element ratios such as Sr/Y and Zr/Nb are identical for the two locations. If the Patton-Murray Seamounts can be linked to the Cobb hotspot by compositional and geometrical arguments, the discontinuity of the volcanic lineament requires an unusually variable plume flux. Desonie and Duncan (1990) argued that the MORB-like isotopic ratios of the Cobb-Eickelberg basalts could be the result of a weak, intermittent, thermal plume that melts the depleted upper mantle. This model may also apply to the Patton-Murray Seamounts, but isotopic data are necessary to determine if the Patton-Murray basalts are indeed MORB-like.

CONCLUSIONS

Detroit Seamount was volcanically active approximately 81 m.y. ago. Basalts there have tholeiitic (Site 884) and transitional (Site 883) compositions. The position of the Pacific plate above the Hawaiian hotspot is now constrained back to 81 Ma, approximately 15 m.y. earlier than previous data allowed. Previous plate-motion models, based on other seamount chains and extrapolation from younger parts of the Hawaiian-Emperor chain, suggested an age for Detroit Seamount of approximately 65 to 75 Ma. Either the 81 Ma sample is from very early in the history of a volcano that remained active for at least 6 m.y., or the velocity of the Pacific plate relative to the Hawaiian hotspot increased sometime between 81 and 65 Ma.

Chinook Trough was volcanically active approximately 80 m.y. ago, and erupted basalt similar to mid-ocean ridge tholeiites. Drilling at Site 885/886 encountered these Upper Cretaceous basalts, perhaps as a sill, and did not penetrate to underlying Lower Cretaceous seafloor.

The Patton-Murray seamount platform was constructed over a period of at least 10 m.y. (from at least 27 Ma to 17 Ma). These dates are from two compositionally distinct volcanic phases in the upper half of the recovered section, and probably underestimate the volcanic lifespan of this seamount platform. Basalts from the lower part of the recovered section are compositionally indistinguishable from basalts from the Cobb-Eickelberg Seamounts. If the Patton-Murray Seamounts can be linked to the Cobb hotspot by compositional and geometrical arguments, an unusual (thermal?) mantle plume with variable flux and depleted chemistry is required.

ACKNOWLEDGMENTS

We are grateful to Roger Nielsen and Lew Hogan for facilitating the microprobe analyses and Ar analyses, respectively. Brian Hausback and an anonymous reviewer provided helpful reviews of the original manuscript. This work was supported by a grant from JOI-USSAC.

REFERENCES*

Allan, J.F., Chase, R.L., Cousens, B., Michael, P.J., Gorton, M.P., and Scott, S.D., 1993. The Tuzo Wilson volcanic field, NE Pacific: alkaline volcanism at a complex, diffuse, transform–trench–ridge triple junction. *J. Geophys. Res.*, 98:22367–22387.

Castillo, P., Batiza, R., and Stern, R.J., 1986. Petrology and geochemistry of Nauru Basin igneous complex: large-volume, off-ridge eruptions of MORB-like basalt during the Cretaceous. *In* Moberly, R., Schlanger, S.O., et al., *Init. Repts. DSDP,* 89: Washington (U.S. Govt. Printing Office), 555–576.

Chapman, D., Allis, R., Bentowski, W., Bone, M., Cermak, V., Hamilton, T., Lewis, T., McDonald, R., Rohr, K., Seeman, D., Spence, G., Willett, S., and Wright, J., 1987. A geophysical investigation at the southeast terminus of the Kodiak-Bowie seamount chain. *Eos,* 68:1498. (Abstract)

Clague, D.A., and Dalrymple, G.B., 1987. The Hawaiian-Emperor volcanic chain. Part I. Geologic evolution. *In* Decker, R.W., Wright, T.L., and Stauffer, P.H. (Eds.), *Volcanism in Hawaii.* Geol. Surv. Prof. Pap. U.S., 1350:5–54.

Clague, D.A., Fisk, M.R., and Bence, A.E., 1980. Mineral chemistry of basalts from Ojin, Nintoku, and Suiko Seamounts Leg 55 DSDP. *In* Jackson, E.D., Koizumi, I., et al., *Init. Repts. DSDP,* 55: Washington (U.S. Govt. Printing Office), 607–637.

Dalrymple, G.B., Clague, D.A., Vallier, T.L., and Menard, H.W., 1987. $^{40}Ar/^{39}Ar$ age, petrology, and tectonic significance of some seamounts in the Gulf of Alaska. *In* Keating, B.H., Fryer, P., Batiza, R., and Boehlert,

* Abbreviations for names of organizations and publications in ODP reference lists follow the style given in *Chemical Abstracts Service Source Index* (published by American Chemical Society).

G.W. (Eds.), *Seamounts, Islands and Atolls.* Geophys. Monogr., Am. Geophys. Union, 43:297–315.

Dalrymple, G.B., Lanphere, M.A., and Natland, J.H., 1980. K-Ar minimum age for Meiji Guyot, Emperor seamount chain. *In* Jackson, E.D., Koizumi, I., et al., *Init. Repts. DSDP,* 55: Washington (U.S. Govt. Printing Office), 677–683.

Desonie, D.L., and Duncan, R.A., 1990. The Cobb-Eickelberg seamount chain: hotspot volcanism with mid-ocean ridge basalt affinity. *J. Geophys. Res.,* 95:12697–12711.

Duncan, R.A., 1991. Age distribution of volcanism along aseismic ridges in the eastern Indian Ocean. *In* Weissel, J., Peirce, J., Taylor, E., Alt, J., et al., *Proc. ODP, Sci. Results,* 121: College Station, TX (Ocean Drilling Program), 507–517.

Duncan, R.A., and Clague, D.A., 1985. Pacific plate motion recorded by linear volcanic chains. *In* Nairn, A.E.M., Stehli, F.G., and Uyeda, S. (Eds.), *The Ocean Basins and Margins* (Vol. 7A): *The Pacific Ocean:* New York (Plenum), 89–121.

Duncan, R.A., and McDougall, I., 1976. Linear volcanism in French Polynesia. *J. Volcanol. Geotherm. Res.,* 1:197–227.

Fleck, R.J., Sutter, J.F., and Elliott, D.H., 1977. Interpretation of discordant $^{40}Ar/^{39}Ar$ age-spectra of Mesozoic tholeiites from Antarctica. *Geochim. Cosmochim. Acta,* 41:15–32.

Forsythe, L.M., and Fisk, M.R., 1994. Comparison of experimentally crystallized and natural spinels from Leg 135. *In* Hawkins, J., Parson, L., Allan, J., et al., *Proc. ODP, Sci. Results,* 135: College Station, TX (Ocean Drilling Program), 585–594.

Geist, D.J., McBirney, A.R., and Duncan, R.A., 1986. Geology and petrogenesis of lavas from San Cristobal Island, Galápagos Archipelago. *Geol. Soc. Am. Bull.,* 97:555–566.

Hooper, P.R., 1981. The role of magnetic polarity and chemical analysis in establishing the stratigraphy, tectonic evolution, and petrogenesis of the Columbia River Basalts. *Mem.—Geol. Soc. India,* 3:362–376.

Hurford, A.J., and Hammerschmidt, K., 1985. $^{40}Ar/^{39}Ar$ and K-Ar dating of the Fish Canyon Tuff: calibration ages for fission-track dating standards. *Chem. Geol.,* 58:23–32.

Lanphere, M.A., and Dalrymple, G.B., 1978. The use of $^{40}Ar/^{39}Ar$ data in evaluation of disturbed K-Ar systems. *In* Zartman, R.E. (Ed.), *Short Papers of the Fourth International Conference, Geochronology, Isotope Geology.* Open-File Rep.— U.S. Geol. Surv., 78-701:241–243.

McDougall, I., and Harrison, T.M., 1988. *Geochronology and Thermochronology by the $^{40}Ar/^{39}Ar$ Method:* Oxford (Oxford Univ. Press).

Pollitz, F.F., 1988. Episodic North America and Pacific plate motions. *Tectonics,* 7:711–726.

Rea, D.K., Basov, I.A., Janecek, T.R., Palmer-Julson, A., et al., 1993. *Proc. ODP, Init. Repts.,* 145: College Station, TX (Ocean Drilling Program).

Rea, D.K., and Dixon, J.M., 1983. Late Cretaceous and Paleogene tectonic evolution of the North Pacific Ocean. *Earth Planet. Sci. Lett.,* 65:145–166.

Sager, W.W., and Pringle, M.S., 1988. Mid-Cretaceous to Early Tertiary apparent polar wander path of the Pacific Plate. *J. Geophys. Res.,* 93:11753–11771.

Stewart, R.J., Natland, J.H., and Glassley, W.R., 1973. Petrology of volcanic rocks recovered on DSDP Leg 19 from the North Pacific Ocean and the Bering Sea. *In* Creager, J.S., Scholl, D.W., et al., *Init. Repts. DSDP,* 19: Washington (U.S. Govt. Printing Office), 615–627.

Walker, D.A., and McDougall, I., 1982. $^{40}Ar/^{39}Ar$ and K-Ar dating of altered glassy volcanic rocks: the Dabi Volcanics. *Geochim. Cosmochim. Acta,* 46:2181–2190.

Weis, D., White, W.M., Frey, F.A., Duncan, B., Dehn, J., Fisk, M., Ludden, J., Saunders, A., and Storey, M., 1992. The influence of mantle plumes in generation of Indian Ocean crust. *In* Duncan, R.A., Rea, D.K., Kidd, R.B., von Rad, U., and Weissel, J.K. (Eds.), *The Indian Ocean: A Synthesis of Results from the Ocean Drilling Program.* Geophys. Monogr., Am. Geophys. Union, 70:57–89.

White, W.M., McBirney, A.R., and Duncan, R.A., 1993. Petrology and geochemistry of the Galápagos Islands: portrait of a pathological mantle plume. *J. Geophys. Res.,* 98:19533–19563.

Worsley, T.R., 1973. Calcareous nannofossils: Leg 19 of the Deep Sea Drilling Project. *In* Creager, J.S., Scholl, D.W., et al., *Init. Repts. DSDP,* 19: Washington (U.S. Govt. Printing Office), 741–750.

York, D., 1969. Least-squares fitting of a straight line with correlated errors. *Earth Planet. Sci. Lett.,* 5:320–324.

Date of initial receipt: 5 April 1994
Date of acceptance: 17 October 1994
Ms 145SR-131